GEOPHYSICAL RESEARCH LETTERS, VOL. 25, NO.14, PAGES 2585-2588, JULY 15, 1998

The auroral oval boundaries on January 10, 1997: A comparison of global magnetospheric simulations with UVI images

R. K. Elsen,[1] R. M. Winglee,[1] J. F. Spann,[2] G. A. Germany,[3]
M. Brittnacher,[1] and G. K. Parks[1]

Abstract. We present a global magnetospheric simulation of the initial period of the January 10–11, 1997 magnetic cloud event. Model magnetospheric boundaries mapped to the ionosphere are compared to UVI images of the auroral oval from 1:00 to 4:30 UT. The convection reversal boundary generally matches the UVI equatorward boundary and is almost always poleward of the boundary separating Region 1 and Region 2 currents. The separatrix between open and closed magnetic field lines matches the poleward boundary of the UVI images well during quiet periods. During dynamic periods when the separatrix moves several degrees in latitude in some sectors, the poleward boundary of the Region 1 currents matches the UVI images better.

Introduction

The poleward boundary of the auroral oval confines the polar cap, believed to lie on open field lines that map into the lobes of the magnetotail. Statistical patterns of field-aligned current generally coincide with the auroral oval [e.g., *Iijima and Potemra*, 1978]. Auroral electron precipitation probably carries most upward currents in the oval, i.e., the duskside Region 1 and dawnside Region 2 current systems, while downward currents in the oval may be carried by upward moving thermal electrons from the ionosphere [*Anderson and Vondrak*, 1975]. Another system of field-aligned currents poleward of the Region 1 currents, designated NBZ or "Region 0" currents, are often observed in the polar cap during periods of northward IMF [*Iijima et al.*, 1984]. *Coley* [1983] found a general collocation in both the morning and evening sectors of the poleward boundary of field-aligned currents, the precipitation boundary for 1 keV electrons, and the convection reversal boundary in the ionosphere marked by the separation of sunward and antisunward flow. These poleward boundaries often agree well but sometimes show significant disagreement, especially during substorm periods [*Lopez et al.*, 1992].

Many boundaries demarcating the magnetospheric plasma regions associated with the auroral oval are self-consistently generated by global magnetospheric simulations, providing an independent test of the location of these boundaries relative to observed auroral oval boundaries. Global simulations produce the magnetic topology of the magnetosphere for different orientations of the IMF, giving the separatrix between open and closed magnetic field lines; the boundaries of all three large-scale, directly-driven field-aligned current systems (NBZ or Region 0, Region 1, and Region 2); and the convection reversal boundary of a global convection pattern. We present a simulation of the initial period (01–05 UT) of the January 10–11, 1997 magnetic cloud event. This period had continuous imaging of the auroral oval by the Ultraviolet Imager (UVI) on the Polar spacecraft [*Torr et al.*, 1995]. The present work compares the boundaries self-consistently generated in the global simulation with the poleward and equatorward boundaries observed by UVI from 1:00 to 4:30 UT.

Simulation and Results

The global magnetospheric simulation used the modified fluid model of *Winglee et al.* [1998]. The simulation box extends sunward to +30 R_E, tailward to -102 R_E, and on the flanks to $\pm 45 R_E$ and uses non-uniform Cartesian grid spacing with a grid resolution of 0.44 R_E in the inner magnetosphere, where the inner radius is set at 2.7 R_E. The simulation ran from 0:00 to 5:00 UT using solar wind plasma and IMF data from Wind [Figure 1], upstream at [85, -57, -16] R_E (GSM).

The shock propagation time to the magnetosphere in the simulation ($\sim$ 15 min, verified with Geotail data) changed little during the study period. A uniform time delay of 15 minutes has been added to give Convected Universal Time (CUT) in Figure 1 for comparison of simulation results and UVI images. Density and velocity jumps at 1:06 CUT indicate shock arrival at the magnetosphere (00:51 UT at Wind). Weak northward IMF (+1 nT) had produced a very quiet magnetosphere prior to shock arrival, but increases to strong values for about an hour. IMF B_Y polarity is almost always positive after 1:50 CUT. The IMF abruptly turns south at 2:20 CUT, producing an 80-min growth phase before substorm onset imaged by UVI at 3:34 UT. The magnetic cloud finally arrives just before 5:00 CUT.

By 1:13 UT the shock wave has progressed to about 20 R_E in the tail and compressed magnetic field lines

[1] Geophysics Program, University of Washington, Seattle, WA
[2] NASA Marshall Space Flight Center, Huntsville, AL
[3] University of Alabama, Huntsville, AL

Paper number 98GL01066.
0094-8534/98/98GL-01066$05.00

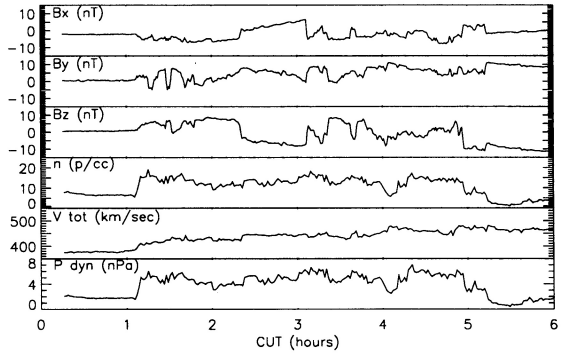

Figure 1. Solar wind parameters measured at Wind from 0–5 UT: from top to bottom, the three IMF components, plasma density and total velocity, and dynamic pressure. A constant 15-min time delay from Wind gives time scale in Convected UT (CUT).

threading the plasma sheet at midnight. Shock-induced precipitation has illuminated the auroral oval at most azimuth angles (Figure 2, converted into MLT coordinates), but precipitation is very weak in the midnight and evening sectors. Strong dipole tilt (near $-30°$ during the study period) means the northern oval is completely free of UV dayglow. Thick oval boundaries ($\sim 10°$) on the dayside surround a tear-shaped polar cap devoid of precipitation.

Figure 3a shows diagnostics from the simulation at 1:12.5 UT. Color contours indicate field-aligned current density as mapped to the northern ionosphere. The Region 1 current system generally lies where UV emissions are observed, and like the particle precipitation, is stronger on the dawn side (red-yellow-gray) than the dusk side (purple-blue-green). Only dawnside Region 1 current exceeds the contour threshold of 0.15 $\mu A/m^2$. Weak Region 2 currents lie equatorward with a sense opposite the Region 1 currents. Strong NBZ or "Region 0" currents, also with a sense opposite the Region 1 currents, are seen poleward of the Region 1 currents, and their high magnitudes can be attributed to the northward IMF. A significant fraction of the dawnside Region 1 current closes through the dawnside Region 0 current, permitting the duskside current systems to be weaker. Dawn-dusk asymmetry, mostly from persistent positive

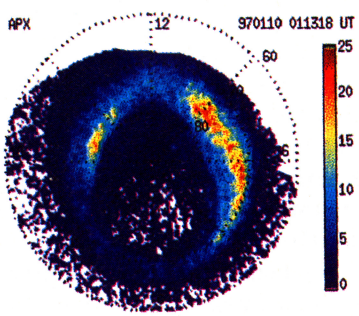

Figure 2. Polar UVI image of auroral oval at 1:13:18 UT, converted to MLT coordinates. False color shows UV photon flux in this 36-sec LBHL image, with each count proportional to a brightness of 25–30 Rayleighs.

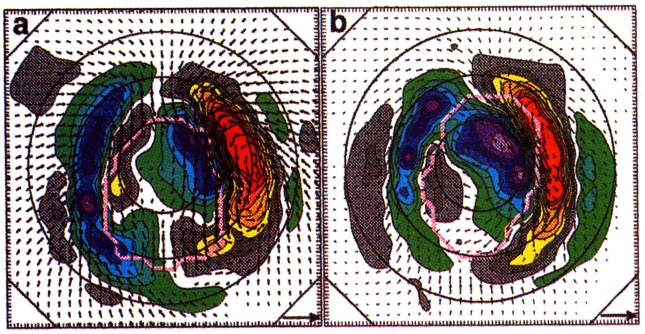

Figure 3. (a) Global simulation diagnostics at 1:12.5 UT mapped down to northern ionosphere. Noon is at top, circles show 10° increments of latitude. Contour levels of downward current (red-yellow-gray) and upward current (purple-blue-green) are steps in current density of 0.02 $\mu A/m^2$. The pink line is magnetic separatrix between open and closed field lines. Plasma convection velocities (overlaid arrows) scale like the bold arrow in the lower right hand corner with a magnitude of 1.4 km/sec. (b) Same simulation diagnostics at 2:30.0 UT, with the same contour levels and arrow scaling.

IMF B_Y, is much weaker than north-south asymmetry from dipole tilt.

The separatrix between open and closed magnetic field lines (heavy pink line) lies just poleward of most of the Region 1 current. A magnetic field line is considered "open" if it does not return to the Earth within the simulation box. The large box size minimizes the misidentification of lines which might otherwise close at larger distances in an even bigger simulation box. Most of the Region 1 (Region 0) currents lie outside (inside) the magnetic separatrix, putting these currents largely on closed and open field lines, respectively. Despite this topology, some open field lines thread the plasma sheet, strongly warped by dipole tilt.

We now compare these simulation boundaries to the poleward edge of the UV oval (Figure 2), which roughly follows 80° latitude sunward of the dawn-dusk meridian but reaches to 70° at midnight. There is no distinct boundary to the Region 1 currents where they vanish near noon and midnight, but the poleward boundary is well defined on the dawn and dusk flanks by a strong gradient. While the poleward boundary of the Region 1 currents is very roughly coincident with the observed

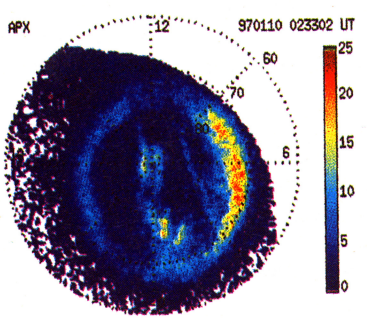

Figure 4. Polar UVI image at 2:33:02 UT with extensive polar cap precipitation.

polar cap on much of the dawn and dusk flanks, there are differences ($> 5°$) at some locations, even if we ignore areas adjacent to noon and midnight where there are no strong gradients. On the other hand, the magnetic separatrix is well defined at all local times and during this quiet period provides a very good fit with the observed poleward boundary at all local times (within $\sim 2°$). As expected, essentially all of this initial auroral precipitation occurs on closed field lines so nearly all of the observed polar cap is threaded by open field lines.

The convection pattern in the northern hemisphere mapped down to the ionosphere along dipole magnetic field lines (arrows in Figure 3a) is a two-cell convection pattern with no sunward flow inside the magnetic separatrix. The convection reversal boundary (CRB) can be identified by regions of high velocity shear on the dawn and dusk flanks, where the Region 1 current is maximum and some flow velocities are near 1 km/sec. There is also a reversal of flow direction normal to and slightly equatorward of the separatrix in the midnight sector, but there is no flow reversal near noon. The CRB lies fairly close to the equatorward edge of the imaged oval at many local times. It lies a few degrees poleward of the imaged edge on the dayside and fits even better on the nightside.

The Region 2 currents all fall well equatorward of the observed precipitation. Even the equatorward Region 1 boundary, defined here to be just inside the regions of strong gradient, falls a few to several degrees below the precipitation boundary at all local times. The simulation indicates nearly all of the auroral precipitation lies in areas of Region 1 current. This pattern is consistent with energetic electron precipitation producing both an upward (Region 1) current and UV emissions on the dusk side of the auroral oval. On the dawnside, however, the electron precipitation is not in the Region 2 area, as expected from the statistical patterns of *Iijima and Potemra* [1978], but rather is collocated with upward moving (presumably thermal) electrons that produce the dawnside Region 1 currents.

Figure 4 shows a UVI image from 2:33 UT, a few minutes after a faint transpolar arc connects heavy polar cap precipitation near midnight to the dayside oval and another arc emerges from the dawn flank of the auroral oval. This is $\sim$ 13 minutes after an abrupt reversal to southward IMF (while IMF B_Y stays positive) has reached the magnetosphere (Figure 1). Figure 3b shows the field-aligned currents, magnetic separatrix, and ionospheric convection velocity from the simulation at 2:30.0 UT. The Region 1 current system is growing strongly following the southward turning at 2:20 UT and is still roughly collocated with the strong dawnside precipitation. Again, the dawnside Region 1 and Region 0 currents are stronger than those on the duskside and, like the precipitation, will remain so for most of the simulation period. The duskside Region 0 currents have become very weak following the southward turning and are actually replaced on parts of the dusk dayside by upgoing currents. This extension of the dawnside Region 0 connects to the duskside Region 1 current. Thia feature makes boundary identification difficult near 15 MLT and is not present in statistical patterns of field-aligned current [e.g., *Iijima and Potemra*, 1978; *Iijima et al.*, 1984]. The Region 2 currents are now stronger and all current systems, which have moved poleward during the extended period of strong northward IMF, are now slowly beginning to move southward.

The separatrix is now rapidly moving equatorward following the IMF B_Z reversal, especially from 9 to 12 MLT, due to vigorous dayside reconnection. Different and sometimes opposing motions of the separatrix at different local times is qualitatively similar to the motion of poleward oval boundary described by *Kamide et al.* [1997]. The ionospheric convection pattern, which by 1:30 UT had developed a 4-cell pattern with sunward flow and counter-rotating cells at high latitudes, is now beginning to revert back to a 2-cell convection pattern. Strong antisunward flow of reconnected flux is seen on the dawn side. The remaining sunward flow inside the separatrix is mostly limited to the dusk dayside.

While the separatrix matches the UV oval well from 14 to 24 MLT (polar cap precipitation prevents a good comparison from 0 to 6 MLT), it does not match the UV oval well from 6 to 14 MLT. Rather the poleward boundary of the Region 1 current, which moves much less than the separatrix, matches better from 6 to 11 MLT. The CRB still gives a fairly good fit to the imaged equatorward boundary at all local times, within a few degrees but slightly poleward (equatorward) on the dawn (dusk) side. Again virtually all of the precipitation (excluding that in the polar cap) falls in Region 1 current areas on both the dawn and dusk sides with no precipitation seen in the Region 2 areas. The simulation predicts that essentially all of the polar cap precipitation, including the transpolar arcs, lies on open field lines, not only at 2:30, but generally from 1:50 to 3:00 when extensive polar cap precipitation was observed.

Time History Behavior

We have measured these boundaries in the simulation and the UVI images at eight local times around the oval every 5 minutes from 1:00 to 4:30 UT. The poleward boundary comparison is shown in Figure 5a and the equatorward boundary comparison in Figure 5b. The UVI boundary (solid line) was determined every 3 minutes by applying a threshold of 8 photons/cm^2/sec (corresponding to a brightness of 200–250 Rayleighs at 170 nm) to the 36-second images from the LBHL filter. This threshold provides an uncertainty of $\sim 1°$ in the measurements when the observed boundary is sharp, but larger uncertainties up to several degrees when UV emissions are faint or lacking a steep gradient. While this provided a good way to define the equatorward boundary, the polar cap precipitation exhibited large latitude excursions at 0 MLT from 1:30 to 3:00 UT and lesser excursions at 21 and 3 MLT. The uncertainty in the measured simulation boundaries, determined by the mapping to 1 R_E from adjacent grid points at 4.4 R_E where the diagnostics are calculated, is about 2°.

The separatrix had closed up significantly during the hour of strong northward IMF and reaches a minimum

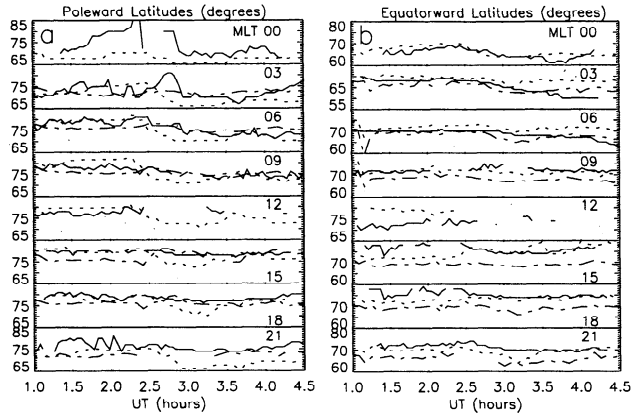

Figure 5. UVI oval boundaries compared to global simulation boundaries, measured from 1:00 to 4:30 UT at eight magnetic local times, from 0 MLT at top down to 21 MLT. (a) Poleward auroral oval boundary (solid line), magnetic separatrix (dotted line), and poleward boundary of the Region 1 currents (dash-dot line). (b) Equatorward auroral oval boundary (solid line), convection reversal boundary (dotted line), and equatorward boundary of the Region 1 currents (dash-dot line).

size near 2:15 UT. The separatrix lies somewhat poleward of the observed polar cap on the dawn side, especially at 9 MLT, but still lies close to the observed boundary along most of the dusk side. In fact, the separatrix (dotted line, Figure 5a) often fits the UVI poleward boundary very well at many locations during the period of northward IMF, e.g. at 6, 15, and 18 MLT from 1:00 to 2:20 UT, and would fit better at 0, 3, and 21 MLT if polar cap precipitation were ignored. Within $\sim$ 30 minutes of the southward turning, however, the separatrix moves significantly equatorward of the UV boundary at all local times. Surprisingly, at about this time the poleward Region 1 boundary (dashed line), which until now did not fit very well, has become a good fit to the UV boundary at many locations on both the dawn and dusk sides, e.g. at 6, 9, 15, and 18 MLT, and generally remains so through the substorm period until 4:30 UT. Thus, while no single model boundary fits all the observations well at all times, the magnetic separatrix is better during quiet times (and northward IMF B_Z) while the Region 1 boundary fits better during active times (and southward IMF B_Z). This general coincidence of the poleward boundary of the Region 1 currents with the UV boundary (and thus the keV electron precipitation boundary) is consistent with the results of *Coley* [1983]. Simply assuming that all of the polar cap is on open lines and all of the auroral emissions are on closed lines may be justified during quiet, steady-state conditions, but may not be valid during dynamic times when the magnetic topology is rapidly changing.

The convection reversal boundary (dotted line, Figure 5b) provides a relatively good fit for the equatorward boundary at some locations, e.g. 0 and 9 MLT, for the entire comparison period, for both northward and southward IMF. Other fits are good only during northward IMF, e.g. 3 MLT, or southward IMF, e.g. 15 and 18 MLT. While *Coley* [1983] found the CRB was generally located with the poleward precipitation boundary, we find that the CRB is almost always well equatorward of this location such that it fits the equatorward precipitation boundary better. The equatorward Region 1 boundary (dashed line) is usually significantly below the equatorward UV boundary at most local times, although these boundaries often match well at 6 MLT and sometimes at 3 MLT. Thus, the precipitation region almost always terminates poleward of the Region 1 boundary with limited reaches across this boundary into the Region 2 area, most notably at 3 MLT shortly after substorm onset (3:34 UT).

This study has found good comparisons between UVI images and some of the boundaries self-consistently generated in global magnetospheric models. While many of the results were expected, some were not. These include the occurrence of the dawnside auroral precipitation in the Region 1 zone, the general collocation of the CRB with the equatorward UV boundary, and the transient departure of the magnetic separatrix from the imaged polar cap when the lesser motion of the Region 1 current boundaries provides a better fit. To test if such boundary collocations generally hold, other periods with UVI observations should be modeled. Future studies could investigate the physical causes of these unexpected results and also include field line mapping from the points on the UVI images or from simulation boundaries to find their magnetospheric sources.

Acknowledgments. This work was supported in part by NASA research grants NAG5-3170 and NAGW 5047.

References

Anderson, H. R., and R. R. Vondrak, Observations of Birkeland currents at auroral latitudes, *Rev. Geophys. Space Phys.*, *13*, 243, 1975.

Coley, W. R., Spatial relationship of field-aligned currents, electron precipitation, and plasma convection in the auroral oval, *J. Geophys. Res.*, *88*, 7131, 1983.

Iijima, T., and T. A. Potemra, Large scale characteristics of field-aligned currents associated with substorms, *J. Geophys. Res.*, *83*, 599, 1978.

Iijima, T., et al., Large-scale Birkeland currents in the dayside polar region during strongly northward IMF–A new Birkeland current system, *J. Geophys. Res.*, *89*, 7441, 1984.

Kamide, Y., et al., The size of the polar cap as an indicator of substorm energy, *Phys. Chem. Earth*, in press, 1997.

Lopez, R. E., H. E. Spence, and C.-I. Meng, Substorm aurorae and their connection to the inner magnetosphere, *J. Geomag. Geoelectr.*, *44*, 1251, 1992.

Torr, M. R., et al., A far ultraviolet imager for the international solar-terrestrial physics mission, *Space Sci. Rev.*, *71*, 329, 1995.

Winglee, R. M., et al., Flux rope structures in the magnetotail: Comparison between Wind/Geotail observations and global simulations, *J. Geophys. Res.*, *103*, 135, 1998.

R. K. Elsen, R. M. Winglee, M. Brittnacher, G. K. Parks, Geophysics Program, Box 351650, University of Washington, Seattle, WA 98195 (e-mail: elsen@geophys.washington.edu).

J. F. Spann, Space Sciences Laboratory, NASA Marshall Space Flight Center, Huntsville, AL 35812.

G. A. Germany, Center for Space Plasma and Aeronomic Research, University of Alabama, Huntsville, AL 35899.

(received December 2, 1997; revised February 24, 1998; accepted March 13, 1998.)